Aalborg Universitet

Automatic Detection of Inactive Solar Cell Cracks in Electroluminescence Images

Spataru, Sergiu; Hacke, Peter; Sera, Dezso

Published in:
Proceedings of the 44th IEEE Photovoltaic Specialists Conference, PVSC 2017

DOI (link to publication from Publisher):
10.1109/PVSC.2017.8366106

Publication date:
2017

Document Version
Accepted author manuscript, peer reviewed version

Link to publication from Aalborg University

Citation for published version (APA):
Spataru, S., Hacke, P., & Sera, D. (2017). Automatic Detection of Inactive Solar Cell Cracks in Electroluminescence Images. In *Proceedings of the 44th IEEE Photovoltaic Specialists Conference, PVSC 2017* (pp. 1421-1426). IEEE Press. I E E E Photovoltaic Specialists Conference. Conference Record https://doi.org/10.1109/PVSC.2017.8366106

General rights
Copyright and moral rights for the publications made accessible in the public portal are retained by the authors and/or other copyright owners and it is a condition of accessing publications that users recognise and abide by the legal requirements associated with these rights.

- Users may download and print one copy of any publication from the public portal for the purpose of private study or research.
- You may not further distribute the material or use it for any profit-making activity or commercial gain
- You may freely distribute the URL identifying the publication in the public portal -

Take down policy
If you believe that this document breaches copyright please contact us at vbn@aub.aau.dk providing details, and we will remove access to the work immediately and investigate your claim.

Downloaded from vbn.aau.dk on: August 26, 2022

Automatic Detection of Inactive Solar Cell Cracks in Electroluminescence Images

Sergiu Spataru[1], Peter Hacke[2], Dezso Sera[1]

[1]Aalborg University, Aalborg, 9220, Denmark
[2]National Renewable Energy Laboratory, Golden, CO 80401, United States

***Abstract* — Inactive solar cell regions resulted from their disconnection from the electrical circuit of the cell are considered to most severe type of solar cell cracks, causing the most power loss. In this work, we propose an algorithm for automatic determination of the electroluminescence (EL) signal threshold level corresponding these inactive solar cell regions. The resulting threshold enables automatic quantification of the cracked region size and estimation of the risk of power loss in the module.**

We tested the algorithm for detecting inactive cell areas in standard mono and mc-Si, showing the influence of current bias level and camera exposure time on the detection. Last, we examined the correlation between the size of the detected solar cell cracks and the power loss of the module.

***Index Terms* — crystalline silicon, cell crack, detection, diagnosis, electroluminescence, photovoltaic module.**

I. Introduction

Solar cell micro-cracks can occur due to mechanical stress during the PV panel manufacturing process [1], transportation [2], or installation [3]. It is estimated that ~6% of PV panels develop at least one crack after transportation [4]. These can further evolve, or new ones can be formed during the service of the PV module due to wind or snow loads [5] and temperature cycling [6]. The most severe cracks can cause significant power loss [7], as well as hot-spots [3], which can further shorten the lifetime of the PV panel.

Currently, the most efficient method of solar cell crack detection is electroluminescence (EL) imaging. Nowadays, EL cameras have become widespread, and are starting to be used as field diagnostic tools as well on fixed [8] or mobile [9] imaging platforms. Consequently, machine analysis methods for detecting and evaluating the severity of solar cell cracks are valuable for analyzing a large volume of EL image data from a PV plant, for example.

Previous research on investigating the severity of solar cell cracks [10] has defined three main types: mode A, B, and C. Amongst these, mode C cracks – corresponding to inactive cell areas – cause the most power loss in PV modules [10] and have the highest likelihood of causing hot spots. Thus, EL image machine analysis methods need to be able to detect and quantify such severe solar cell cracks.

In [11] a method was proposed for quantifying mode B and C cracks from EL images, based on analyzing the EL intensity distribution of individual cells or the entire PV panel. The method makes use of certain EL intensity thresholds in the image, determined by image segmentation algorithms, or manually from the image. These thresholds determine which areas of the cell correspond to cracks and which are undamaged. This method was included in the draft of the new EL imaging standard currently under development "IEC TS 60904-13 Electroluminescence of photovoltaic modules," which focuses on EL imaging requirements, procedures, and methods for quantification of cell characteristics.

This paper continues that work, and proposes an algorithm for determining the EL intensity threshold corresponding to mode C cracks. This algorithm can be used to automatically detect mode C cracks in low-current bias EL images, as well as for detecting *possible* mode C cracks in high-current bias EL images. Detecting such cracks from high-current bias EL images is relevant for applications that may be constrained by a short imaging exposure time, such as outdoor imaging [12].

In the experimental part of this work we apply the method to detect and quantify cell cracks from mono- and mc-Si PV modules, degraded through accelerated thermo-mechanical stress. In this analysis, we investigate the influence of the forward current bias and camera exposure time used for the PV module EL imaging, on the cell crack detection accuracy of the method. Last, we examine the correlation between the size of the detected solar cell cracks and the power loss of the module. This opens the possibility for estimating the power degradation of a module due to cell cracks from EL images alone, which has potential applications in outdoor EL inspection of PV plants.

II. Types of Solar Cell Cracks

Mode A cracks, shown in Fig. 1a and Fig. 1c, represent an incipient form of solar cell cracks, that usually do not cause much power loss, but can develop over time into more severe type of cell cracks (mode B and C) [10]. The second type of cell cracks, denoted mode B, shown in Fig. 1b and Fig. 1d, correspond to partially disconnected cell areas, that cause increased series resistance and losses [10]. These appear black or gray in the EL images, depending on current-bias of the module and camera exposure time.

The most severe type of cracks is considered mode C, shown in Fig. 1d. These correspond to completely disconnected cell areas [10], effectively reducing the area of the cell and its current generation, and causing the most power loss. Mode C cracks appear black in EL images irrespective of current level and camera exposure time, since no photons are being emitted from the affected regions.

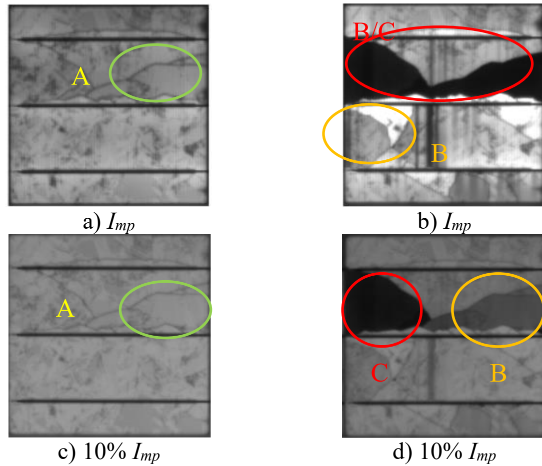

a) I_{mp} b) I_{mp} c) 10% I_{mp} d) 10% I_{mp}

Fig. 1. Example of mode A, B and C solar cell cracks as defined in [10]. EL images correspond mc-Si solar cell before and after thermo-mechanical stress testing: a) mode A crack measured at I_{mp} bias b) mixed mode B/C cracks measured at I_{mp} bias, c) mode A crack at 10% I_{mp} current bias, d) mode B, C cracks measured at 10% I_{mp} bias.

Discerning between mode B and C cracks requires imaging at a low-current bias [10], typically ~10% of the PV module short-circuit (I_{sc}) or maximum power point current (I_{mp}). At these lower current levels, voltage losses due to series resistance (R_s) are smaller, thus mode B cracks, which cause increased R_s, appear relatively brighter relative to the surrounding cell area than in the higher current bias images. On the other hand, mode C cracks remain dark irrespective of the current level. In practice, mode C cracked regions usually have a higher than zero EL intensity due to the noise of the camera, ambient, and reflections from adjacent cells [11].

Most often PV modules are imaged at I_{sc} or I_{mp} bias, to shorten camera exposure time and improve the signal-to-noise ratio of the image. Under these conditions, severe mode B cracks appear the same as mode C in the image, as shown in Fig. 1b. This is due to the low EL signal emission of the cracked area and the limited dynamic range of the camera. We denote this type as *mixed mode B/C cracks* for the rest of the paper.

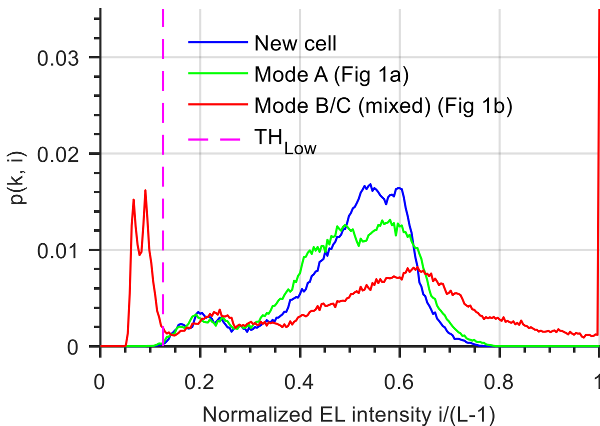

Fig. 2. EL intensity histogram of a solar cell (Fig. 1) imaged at I_{mp} bias, and at different stages of mechanical degradation: blue – new cell; green – affected by mode A cracks (Fig. 1a); red – affected by mode B/C cracks (Fig. 1b).

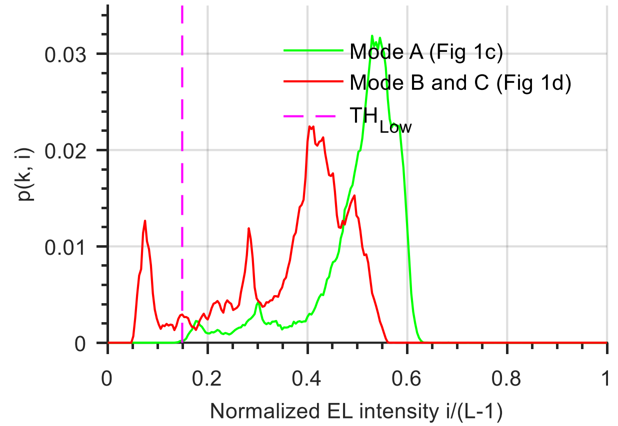

Fig. 3. EL intensity histogram of the solar cell in Fig. 1 imaged at 10% I_{mp} bias, and two stages of degradation: green – affected by mode A cracks (Fig. 1c); red – affected by mode B and C cracks (Fig. 1d).

III. Detection of Mixed Mode B/C and Mode C Solar Cell Cracks

Mixed mode B/C and C cracks can be detected and quantified from the *EL intensity (ELI) histogram* of PV module or of individual cells, as proposed in [11]. The method requires the calculation of a normalized ELI histogram $p(k, i)$, as in (1):

$$p(k,i) = \frac{n_i^k}{n^k},\ 0 \le i < L, 1 \le k \le N_c, \tag{1}$$

where k is the solar cell number, N_c is the number of cells in the module, n_i^k is the number of pixels of gray level i in cell k, n^k is the total number of pixels in the image of cell k, and L is the total number of gray levels in the image.

By calculating $p(k, i)$ for the cell shown in Fig. 1, through the different stages of degradation, we can quantify the effect of cell cracks on the EL signal of the cell. Fig. 2 shows the ELI histogram $p(k, i)$ of the cell imaged at I_{mp} bias. Here we can observe that mode A (green) cracks influence the higher ELI region of the histogram, as compared to when the cell was new (blue). Whereas mode B/C cracks (red) impact the lower region of $p(k, i)$. By quantifying this increase in the lower ELI region, we can determine the area of new mode B/C cracks in the cell.

The same increase in the lower ELI region of the histogram, can be observed in Fig. 3, determined from low bias current EL images of the cell. In this case the increase in the lower ELI region is mainly due to the mode C cracks.

Quantifying mixed mode B/C and C cracks from the lower ELI region of the $p(k, i)$ histogram, requires the determination of an ELI threshold TH_{Low} – shown in magenta in Fig. 2 and Fig. 3. This threshold must separate the active (EL emitting) regions of the cell from the inactive ones, and its value is influenced by the noise level the EL image. Fig. 4 exemplifies the application of TH_{Low} (determined manually) for segmenting cell EL images in Fig. 1b and Fig. 1d, and determining the location and area of the mixed mode B/C and C cracks, respectively.

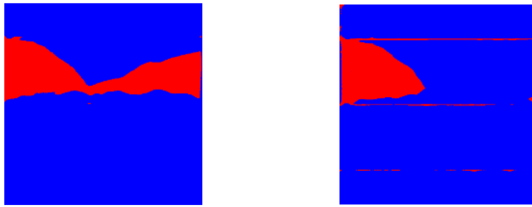

Fig. 4. Binary cell images showing the location of the mode B/C (a) and C cracks (b) segmented from Figs. 1b and 1d, using a threshold TH_{Low} determined manually from the cell ELI histogram $p(k, i)$.

A. Proposed Method for Automatic Determination of TH_{Low}

One of the main challenges in automating the detection and correct quantification of mode B/C and C cracks using the method described in this paper is precisely determining TH_{Low}. Its value is dependent on the current bias level, camera exposure time, ambient noise level, and can even vary slightly from module to module within the same module type. This variation can be observed also in the cell ELI histograms in Fig. 6, between the undamaged cells within the same module. Thus, we need to determine TH_{Low} from each EL image independently, to minimize false detection errors.

In the following, we propose an algorithm for determining TH_{Low} from EL images, which can be used to detect and quantify mode B/C and C cracks, and that can be automated:

1) Select a representative sample (N) of undamaged cells from the module EL image:

Undamaged cells are defined as solar cells with no cracks, shunting or increased series resistance areas. In this work, N=20 (out of 60) cells in the module were selected automatically, based on the criteria of having the lowest standard deviation in the EL intensity histogram. This parameter has been shown to increase with various types of solar cell degradation [13].

2) Select a *WxH* area from each undamaged cell image:

To exclude dark areas, close to the cell edges from affecting the analysis, we recommend performing the TH_{Low} determination only on a central cell area, as depicted in Fig. 5a, corresponding to ~70% width and height.

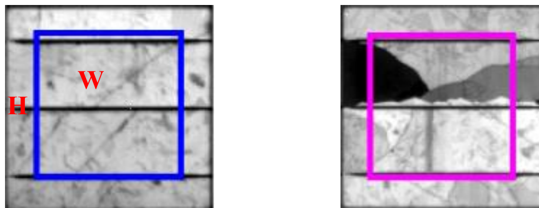

Fig. 5. Example of *WxH* area of analysis (blue), used for determining the low intensity threshold TH_{Low} of the EL Image, for: a) an undamaged cell; b) a cell with mode B and C cracks.

3) Compute the cumulative EL intensity distribution for each area:

For each selected cell image area k, corresponding to the N *undamaged* cells, we compute the cumulative EL intensity distribution $cdp(k, i)$, according to (2):

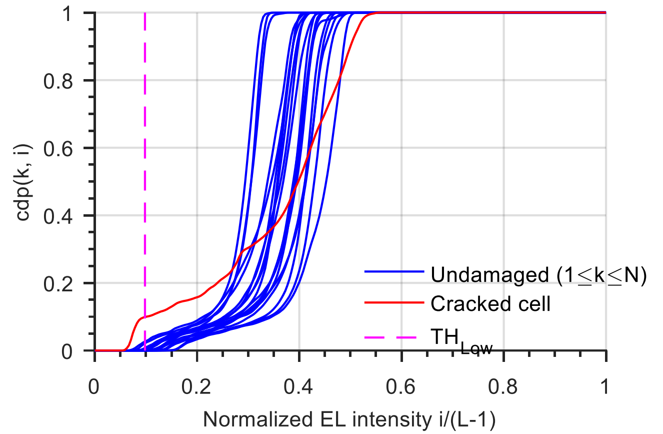

Fig. 6 Cumulative EL intensity profiles for 20 undamaged cells vs. the intensity profile of a cracked cell. The low EL intensity threshold TH_{Low} is calculated from the profile of the undamaged cells.

$$cdp(k,i) = \sum_{j=0}^{i} \frac{n_j^k}{n^k}, 0 \le i < L, 1 \le k \le N \tag{2}$$

Fig. 6 shows the *cdp* distribution for *N=20 undamaged* cells (blue) of a mc-Si module, selected based on the lowest EL intensity standard deviation. By comparison, the *cdp* of a cell with a large mode C crack (Fig. 5b) is shown in magenta. Here we can observe an increase in the number of dark pixels in the image, because of the solar cell crack.

4) Calculate a local threshold for each undamaged cell:

For each $cdp(k, i)$ we calculate a local threshold $TH_{Low}(k)$ as the maximum EL intensity i for which $cdp(k, i)$ is below a fixed threshold A_{IN}:

$$\begin{aligned} TH_{Low}(k) &= max[i] \\ \text{subject to } cdp(k,i) &\le A_{IN} \end{aligned} \tag{3}$$

where A_{IN} is the average percentage of inactive area in an undamaged cell, and is determined primarily by the number thickness of the cell busbars, size of the *WxH* area and camera resolution. AIN must be calibrated for the solar cell type and camera setup. In this work, A_{IN} = 0.1% for mc-Si cells and A_{IN} = 0.5% for mono-Si cells, which have thicker busbars.

5) Calculate a global threshold for the entire module:

Given there will likely be some variation between ELI histogram and $cdp(k, i)$ of the N selected undamaged cells, as can be observed in Fig. 6, the cell thresholds $TH_{Low}(k)$ will vary as well. Consequently, we need to calculate an average TH_{Low} for the entire module. However, considering that cells with defects and low ELI standard deviation may be falsely selected as "undamaged", which will skew the distribution of cell thresholds, the module level threshold TH_{Low} should be calculated as the median of the N local threshold values $TH_{Low}(k)$:

$$TH_{Low} = median\left(TH_{Low}(k)\right) \tag{4}$$

IV. Results and Discussion

To evaluate the mode C crack detection method, we used two sets of standard 60 cell modules (mono- and mc-Si), consisting of four samples each. These were degraded artificially, by several rounds of mechanical loading and humidity freeze cycles, causing the formation of mode A, B, and C cracks. All modules were flash tested under standard test conditions (STC), before and after stress, as well as imaged at 10 % I_{mp} and I_{mp} forward current bias, in a darkroom with a high-resolution Si CCD camera. The mc-Si modules were also imaged at 20% and 50 % I_{mp} bias, as well as two different camera exposures.

A. Influence of Forward Current Bias Level

In the first part of the analysis we investigate the influence of the bias current level during EL imaging on the detection of mode B/C and C cell cracks, in terms of total cracked module area. We applied the algorithm to determine TH_{Low} from each EL image, then the mixed mode B/C and C cracked regions were quantified according to the method described in [11].

Fig. 7 exemplifies the location (in magenta) of the mode C cracks detected from the 10% I_{mp} bias image of one of the mc-Si modules. This solar cell crack map allows for calculating the size of each cracked area isolated from the cell circuit relative to the cell area [11]. Fig. 8 shows the same module, but imaged with I_{mp} bias. Here we can observe a larger number of cell cracks identified as mixed mode B/C, some of which are mode B cracks that show very low EL emission regions, due to the high series resistance, but are not completely disconnected. Nevertheless, they could be considered the most severe mode B cracks in the module based on their low EL emission level.

As can be observed from Fig. 9, the total percent of mode B/C cracks detected per module increases with the module bias-current, which confirms a number of mode B cracked regions confounded as mode C, increases with bias current. This is a limitation of relying on the high-current bias EL images only, where severe mode B cracks will have a similar EL signal level as mode C cracks. Low-bias EL images are necessary to discern between such crack types.

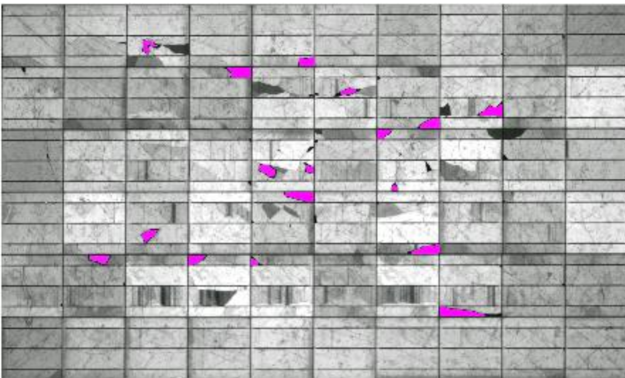

Fig. 7. Low-current bias (10% I_{mp}) EL image of a mc-Si PV module which has sustained thermo-mechanical degradation. The magenta areas represent solar cell cracks that have been identified as Mode C – having an EL intensity below TH_{Low} determined for this bias level.

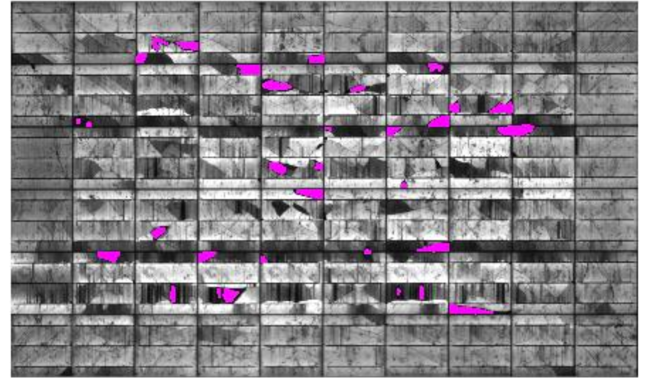

Fig. 8. High-current bias (100% I_{mp}) EL image of a mc-Si PV module in Fig. 7. The magenta areas represent solar cell cracks that have been identified as mixed mode B/C cracks.

B. Artifacts of Camera Exposure Time

In the previous analysis, one of the mono-Si modules was excluded from the analysis because the cell crack detection method –applied to the 10% I_{mp} bias EL image – yielded a cell crack of 100% for one of the cells, which was clearly erroneous. The cause was underexposure of the 10% I_{mp} bias EL image, which had two important consequences. First, image underexposure causes the ELI histogram to skew towards the low EL intensity region, as shown in Fig. 10 (blue), and the cell crack detection is thus confounded by the camera sensitivity and dynamic range. In this situation, determining a valid TH_{Low} threshold to detect mode C cracks is difficult.

The second consequence of EL image underexposure is seen with cells having excessive mode A cracks, as the cell highlighted in Fig. 11 and Fig. 12, measured under 100% and 10% I_{mp} bias, respectively. Typically, cells with a high series resistance will appear brighter (relative to the other cells in the PV module) in low bias images than in higher bias images. However, if the low bias image is underexposed, cells with excessive micro-cracks, causing additional shunting, can appear darker still, due to the voltage losses associated with recombination currents at the cracks and limited dynamic range of the camera.

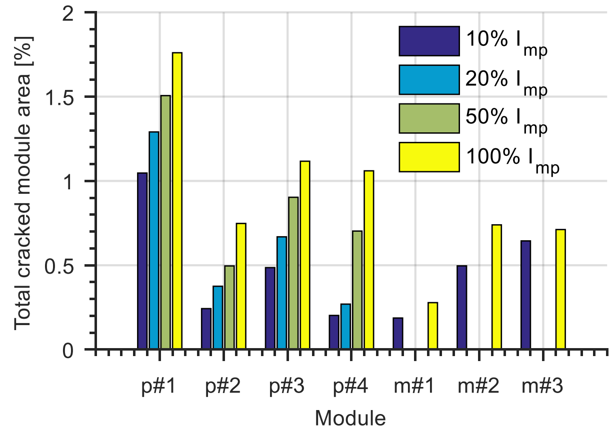

Fig. 9. Percent of mode B/C and C cell cracks relative to the PV module area, for the mc-Si (p#) and mono-Si (m#) modules, determined under different current bias levels.

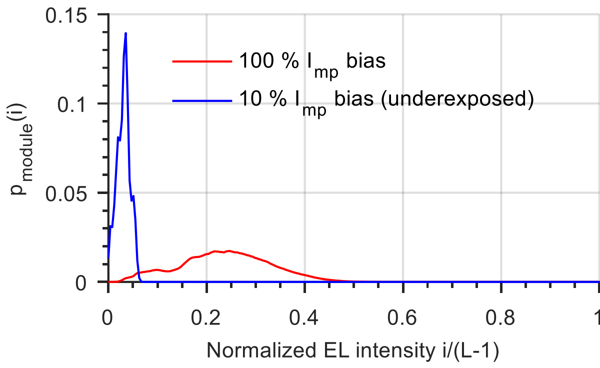

Fig. 10. Normalized ELI histograms of mono-Si module m#4, calculated from EL images measured under I_{mp} (red) and 10% I_{mp} bias (blue) – showing the consequence of image underexposure.

To investigate further the influence of camera exposure time on the cell crack detection method, we analyzed the EL images of the mc-Si modules, measured at I_{mp} bias and two exposure levels (19.2 sec and 25.6 sec). Fig. 13 shows the largest cell crack (relative to cell area) detected in each of the four modules, for the two exposure levels. As can be observed, the differences are negligible – showing that the TH_{Low} calculation method is robust to camera exposure time, if the EL image is not under- or over-exposed.

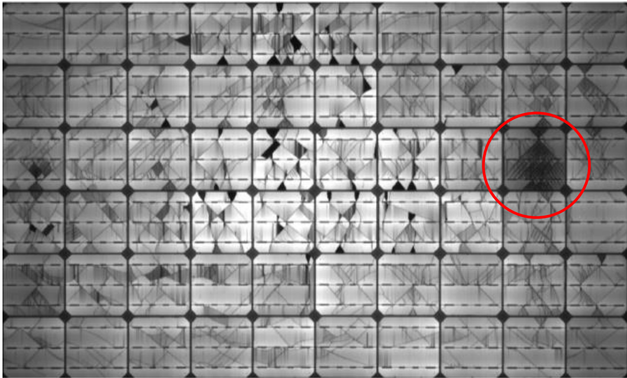

Fig. 11. EL image of module m#4, measured under I_{mp} bias, highlighting a cell with excessive micro-cracks and shunting.

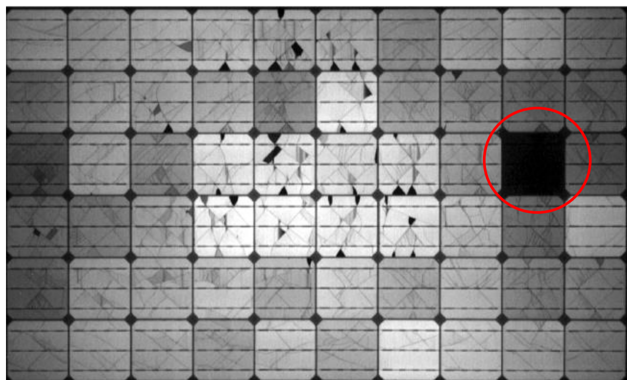

Fig. 12. EL image of module m#4, measured under 10% I_{mp} bias, highlighting a cell with excessive micro-cracks and shunting. The image contrast was adjusted such that the cells are visible.

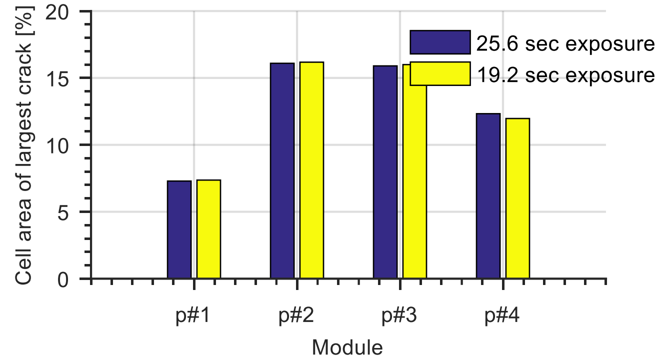

Fig. 13. Largest mode B/C cell cracks relative to the cell area, for the mc-Si modules, measured under two camera exposure and I_{mp} bias.

C. Correlation of Cell Crack Size with Module Power Loss

From a module power loss perspective, mode C cracks are considered severe since they reduce the effective photon collection area of the cell, causing current mismatch in the cell substring. The work in [10] showed that a mode C cracked area lower than ~8% of the total cell area does not cause significant STC power loss. However, for mode C cracks between 8% and 50 % disconnected cell area, the module power loss increases approximately linearly to 33% of module STC power, then saturates due to the bypassing of the cell sub-string.

This mode C crack area vs. STC P_{max} loss characteristic is illustrated in Fig. 14 (dotted red line), which has been obtained through LTSpice simulation of a standard 60-cell 250 Wp mc-Si PV module – where the inactive area of one cell has been varied between 0-25%. This characteristic in Fig. 14 gives us an idea of the lower module power loss boundary, given the size of the largest mode C crack area.

In practice however, modules which have large cracks, often have number of smaller ones, which also cause power loss – thus the total module power loss will be grater. We illustrate this characteristic in Fig. 14, where size of the largest mode B/C crack detected from I_{mp} bias images of the mc- and mono-Si modules, are correlated with the respective module power loss.

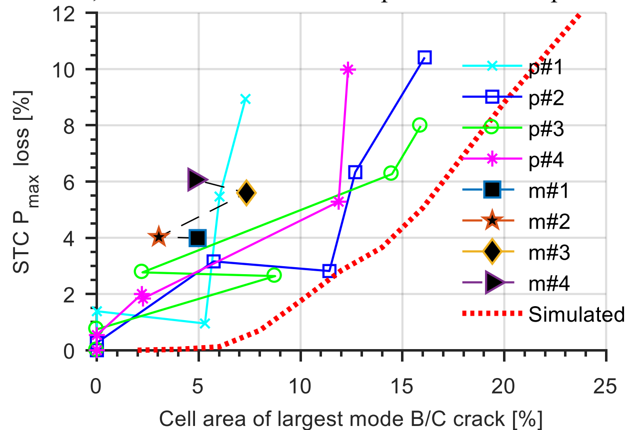

Fig. 14. Largest mode B/C solar cell cracks, measured from I_{mp} bias EL images of the mono- and mc-Si modules, correlated with their respective STC P_{max} degradation due to cracks. Each mc-Si module is imaged at six stages of thermo-mechanical degradation.

Since all the modules have sustained multiple mode B and C cracks, no clear dependency can be observed between the largest mode B/C crack and module power loss. But using the characteristic in Fig. 14 we can infer what is the lower limit of power loss. However, if we calculate the total mode B/C cracked area per module, we can observe a better correlation with module power loss, as shown in Fig. 15.

V. Summary and Conclusion

In this work, we proposed a method to automatically determine the EL intensity threshold necessary for quantifying mode C (inactive) solar cell cracks from low current bias EL images, and mixed mode B/C (appearing inactive) cracks in high current bias EL images. The method was primarily developed to support the mode C solar cell crack quantification method proposed in the draft of the new EL imaging standard currently under development "IEC TS 60904-13 Electroluminescence of photovoltaic modules".

Preliminary results showed that 50-60% of the mixed mode B/C cracks detected in high current bias EL images, overlap with the mode C cracks detected in low current bias EL images. However, this percentage may be lower if the EL image is underexposed, since the detection is limited by the sensitivity and dynamic range of the EL camera.

Last, we showed that the area of mode B/C cracks, detected from high current bias EL images, can be used to approximate the lower module power loss boundary due to cracks. This finding can be relevant for outdoor EL inspection applications, where the EL images are usually taken at higher current bias.

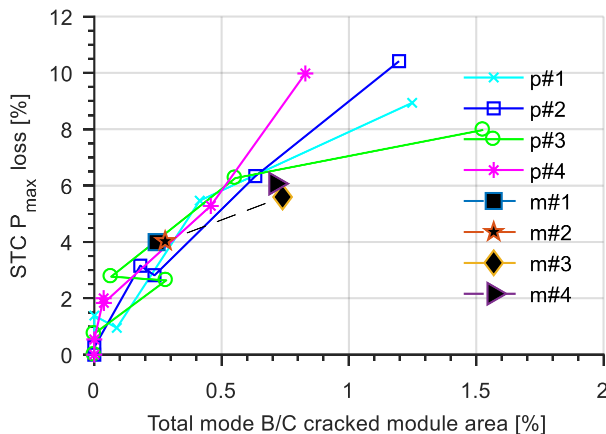

Fig. 15. Total mode B/C cracked module area, measured from I_{mp} bias EL images of the mono- and mc-Si modules, correlated with their respective STC P_{max} degradation due to cracks.

Acknowledgement

The authors thank Karl Bedrich for their help in performing the EL module measurements. This work was partially supported by the research project "DronEL – Fast and accurate inspection of large photovoltaic plants using aerial drone imaging", project 6154-00012B supported by Innovation Fund Denmark, and Aalborg University. As well as financial support from Otto Mønsteds Fond and the U.S. Department of Energy under Contract No. DE-AC36-08-GO28308 with the National Renewable Energy Laboratory.

References

[1] A. M. Gabor, M. Ralli, S. Montminy, L. Alegria, C. Bordonaro, J. Woods, L. Felton, M. Davis, B. Atchley, and T. Williams, "Soldering induced damage to thin Si solar cells and detection of cracked cells in modules," in 21st EUPVSEC, Dresden, Germany, September, 2006, pp. 4-8.

[2] F. Reil, J. Althaus, W. Vaassen, W. Herrmann, and K. Strohkendl, "The Effect of Transportation Impacts and Dynamic Load Tests on the Mechanical and Electrical Behaviour of Crystalline PV Modules," in 25th EUPVSEC, Valencia, Spain, 2010, pp. 3989 - 3992.

[3] M. Köntges, S. Kurtz, C. Packard, U. Jahn, K. A. Berger, K. Kato, T. Friesen, H. Liu, and M. Van Iseghem, *Review of Failures of Photovoltaic Modules*, International Energy Agency, 2014.

[4] M. Köntges, S. Kajari-Schröder, I. Kunze, and U. Jahn, "Crack Statistic of Crystalline Silicon Photovoltaic Modules," in 26th EUPVSEC, Hamburg, Germany, 2011, pp. 3290 - 3294.

[5] S. Kajari-Schröder, I. Kunze, U. Eitner, and M. Köntges, "Spatial and orientational distribution of cracks in crystalline photovoltaic modules generated by mechanical load tests," *Solar Energy Materials and Solar Cells,* vol. 95, no. 11, pp. 3054-3059, 11//, 2011.

[6] M. Sander, S. Dietrich, M. Pander, S. Schweizer, M. Ebert, and J. Bagdahn, "Investigations on crack development and crack growth in embedded solar cells," in Reliability of Photovoltaic Cells, Modules, Components, and Systems Conference, San Diego, California, 2011, pp. 811209-811209-10.

[7] C. Buerhop-Lutz, D. Schlegel, C. Vodermayer, and M. Nieß, "Quality Control of PV-Modules in the Field Using Infrared-Thermography," in 26th EUPVSEC, Hamburg, Germany, 2011, pp. 3894 - 3897.

[8] L. Stoicescu, L. Reuter, and J. Werner, "DaySy: Daylight Luminescence for PV Systems: How to Check 400kWpeak Per Day With Electroluminescence," in 2014 Photovoltaic Module Reliability Workshop, Golden, Colorado, 2014.

[9] S. Koch, T. Weber, T. Sobottka, A. Fladung, P. Clemens, and J. Berghold, "Outdoor Electroluminescence Imaging of Crystalline Photovoltaic Modules: Comparative Study between Manual Ground-Level Inspections and Drone-Based Aerial Surveys," in 32nd EUPVSEC, Munich, Germany, 2016, pp. 1736 - 1740.

[10] M. Köntges, I. Kunze, S. Kajari-Schröder, X. Breitenmoser, and B. Bjørneklett, "The risk of power loss in crystalline silicon based photovoltaic modules due to micro-cracks," *Solar Energy Materials and Solar Cells,* vol. 95, no. 4, pp. 1131-1137, 2011.

[11] S. Spataru, P. Hacke, D. Sera, S. Glick, T. Kerekes, and R. Teodorescu, "Quantifying Solar Cell Cracks in Photovoltaic Modules by Electroluminescence Imaging," in 42nd IEEE Photovoltaic Specialist Conference, New Orleans, 2015, pp. 8.

[12] J. Adams, B. Doll, C. Buerhop-Lutz, T. Pickel, T. Teubner, C. Camus, and C. J. Brabec, "Non-Stationary Outdoor EL-Measurements with a Fast and Highly Sensitive InGaAs Camera" in 32nd EUPVSEC, Munich, Germany, 2016, pp. 1837 - 1841.

[13] S. Spataru, "Characterization and Diagnostics for Photovoltaic Modules and Arrays," Department of Energy Technology, Aalborg university, Aalborg, Denmark, 2015.